PERGAMON

Acta mater. 48 (2000) 3169–3175

Acta MATERIALIA

www.elsevier.com/locate/actamat

EFFECTS OF LINE AND PASSIVATION GEOMETRY ON CURVATURE EVOLUTION DURING PROCESSING AND THERMAL CYCLING IN COPPER INTERCONNECT LINES

T.-S. PARK and S. SURESH†

Department of Materials Science and Engineering, Massachusetts Institute of Technology, Cambridge, MA 02139, USA

(Received 30 December 1999; accepted 17 April 2000)

Abstract—A simple theoretical analysis for curvature evolution in unpassivated and passivated copper interconnect lines on a silicon substrate is proposed. A layer consisting of copper and oxide lines is modeled as a homogenized composite that has different elastic moduli and thermal expansion coefficients in two different directions, i.e. along and across the lines, due to the anisotropic line geometry. These effective thermoelastic properties of the composite layer are approximated in terms of volume fractions and thermoelastic properties of each line using standard composite theory. This analogy facilitates the calculation of curvature changes in Damascene-processed copper lines subjected to chemical–mechanical polishing and/or thermal cycling. The effects of line height, width and spacing on curvature evolution along and across the lines are readily extracted from the analysis. In addition, this theory is easily extended to passivated copper lines irrespective of passivation materials by superimposing the curvature change resulting from an additional layer. Finite element analysis has been used to assess the validity of the theoretical predictions; such comparisons show that the simple theory provides a reasonable match with numerical simulations of curvature evolution during the Damascene process in copper interconnects for a wide range of line and passivation geometry of practical interest.

Keywords: Coating; Composite; Copper; Theory and simulation; Thermal cycling

1. INTRODUCTION

The reliability of metal interconnect lines in integrated circuits is known to be influenced by failure mechanisms such as electromigration [1–3] and stress-induced voiding [4–6]. In ultra large scale integration (ULSI) devices, multilevel metallization is needed. Oxide passivation layer deposition usually involves heating up to 400°C so that the interconnect lines undergo several thermal cycles. Thermal stresses are generated by the large difference in expansion/contraction which develops between the metal interconnect lines and surrounding materials during thermal cycling. Tensile thermal stresses formed during cooling from the oxide deposition temperature can cause voiding near the interface between an interconnect line and the surrounding passivation layer.

Due to the difficulty of etching copper, a new fabrication technique called the Damascene process has been introduced in the semiconductor industry [7]. In this method, trenches whose dimensions conform to the geometry of the copper interconnect lines in the circuit are dry-etched in an oxide layer which is grown on the silicon substrate. These trenches are then plugged with copper by recourse to chemical vapor deposition (CVD) or electroplating. The extra copper above the trenches is then removed by chemical–mechanical polishing (CMP), and then a passivation or capping layer is deposited on top of the interconnect structure. As this process involves polishing, the control of curvature of the silicon wafer becomes critical for uniform polishing over the entire wafer. The changes in curvature induced during polishing and subsequent passivation also provide valuable information about the evolution of internal stresses in the interconnect lines. The objective of this work was to develop a simple theoretical analysis of the evolution of curvature along and across copper interconnect lines on silicon substrates during various fabrication steps, as functions of the line and passivation geometry. The analytical results are verified with numerical simulation using the finite element method

† To whom all correspondence should be addressed.

1359-6454/00/$20.00
PII: S1359-6454(00)00114-2

(FEM) for a range of line geometry of practical interest.

2. ANALYTICAL MODEL

Figure 1(a) is a schematic of Cu interconnect lines on a Si substrate following the Damascene process. Assuming that the aspect ratio (h/w) of the Cu and SiO_2 lines is high (typically equal to or greater than unity), the structure can be homogenized into a composite layer as shown in Fig. 1(b). Due to the anisotropic line geometry, this composite layer has different values of effective elastic modulus and thermal expansion coefficient along the lines, E_x and α_x, respectively, than those across the lines, E_y and α_y, respectively, even if Cu itself is modeled as elastically and thermally isotropic. Using composite theory, these effective properties can be calculated in terms of the volume fraction, elastic modulus and thermal expansion coefficient of Cu lines, f_l ($= w/p$), E_l and α_l, and those of SiO_2 lines, f_o ($= 1 - w/p$), E_o and α_o.

Considering a plate of an elastic material which is subjected to bending moments, M_x and M_y, along the x- and y-directions, respectively, where x–y is the plane of the plate, the resulting non-equibiaxial stresses are generally expressed as [8]

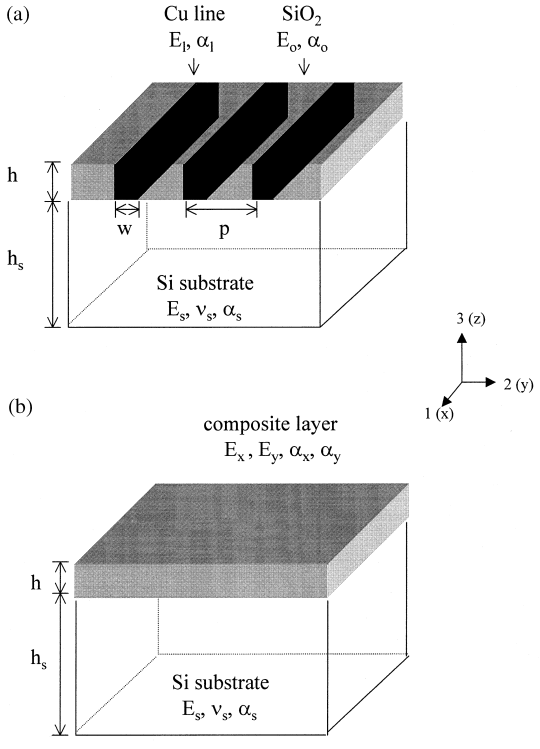

Fig. 1. Schematic of unpassivated Cu interconnect lines on a Si substrate following the Damascene process: (a) individual Cu lines and SiO_2 lines; (b) homogenized composite layer.

$$M_x = \langle\sigma_{xx}\rangle h\left(\frac{h_s}{2}\right) = -\frac{E_s h^3}{12(1-\nu_s^2)}(\kappa_x + \nu_s\kappa_y) \quad (1)$$

$$M_y = \langle\sigma_{yy}\rangle h\left(\frac{h_s}{2}\right) = -\frac{E_s h^3}{12(1-\nu_s^2)}(\kappa_y + \nu_s\kappa_x) \quad (2)$$

where $\langle\sigma_{xx}\rangle$ and $\langle\sigma_{yy}\rangle$ are the normal stresses in the plate along the x- and y-directions, respectively, κ_x and κ_y are the curvatures along the x- and y-directions, respectively, and E_s and ν_s are the elastic modulus and Poisson ratio, respectively, of the Si substrate. Equations (1) and (2) can be rewritten as

$$\kappa_x = -\frac{6}{E_s}\frac{h}{h_s^2}[\langle\sigma_{xx}\rangle - \nu_s\langle\sigma_{yy}\rangle] \quad (3)$$

$$\kappa_y = -\frac{6}{E_s}\frac{h}{h_s^2}[\langle\sigma_{yy}\rangle - \nu_s\langle\sigma_{xx}\rangle]. \quad (4)$$

From equations (3) and (4), it is evident that the curvature in one direction is expected to have some contribution from the thermal stress resulting from thermal mismatch in the other direction. This coupling term, however, includes the Poisson ratio, which makes this contribution relatively small. In addition coupling can be taken into account by considering the effective thermal expansion coefficients of the homogenized composite layer, which somewhat compensates for the limitations of a one-dimensional approach. It could, therefore, be postulated that a simple uniaxial, anisotropic composite model for patterned elastic lines might provide sufficiently accurate predictions of curvature evolution in response to changes in geometry (such as that arising from chemical–mechanical polishing) or to changes in internal stresses arising from thermal cycling. A simple analytical model for curvature evolution, in unpassivated and passivated interconnect lines, is developed on the basis of this premise. The conditions of validity of such a simple model are then assessed using detailed finite element simulations.

The stresses are from thermal mismatch in the uniaxial state is approximated as

$$\begin{aligned}\langle\sigma_{xx}\rangle &= -E_x(\alpha_x - \alpha_s)\Delta T,\\ \langle\sigma_{yy}\rangle &= -E_y(\alpha_y - \alpha_s)\Delta T.\end{aligned} \quad (5)$$

Combining equation (5) with equation (3) or (4), the curvature components are calculated to be

$$\begin{aligned}\kappa_x &= \frac{6}{E_s}\frac{h}{h_s^2}E_x(\alpha_x - \alpha_s)\Delta T,\\ \kappa_y &= \frac{6}{E_s}\frac{h}{h_s^2}E_y(\alpha_y - \alpha_s)\Delta T.\end{aligned} \quad (6)$$

Equation (6), which is valid only for uniaxial loading, is used for calculating curvature evolution of

the homogenized composite layer consisting of Cu and SiO_2 lines which is subjected to biaxial loading.

The volume-averaged stresses from thermal mismatch in the equibiaxial state are expressed as

$$\langle\sigma_{xx}\rangle = \langle\sigma_{yy}\rangle = -\overline{E_f}(\alpha_f - \alpha_s)\Delta T \tag{7}$$

where $\overline{E_f}$ and α_f are the biaxial modulus ($E_f/[1-\nu_f]$) and thermal expansion coefficient, respectively, of a uniform film. Combining equation (7) with equations (3) and (4), the curvatures can be found as

$$\kappa_x = \kappa_y = \frac{6}{\overline{E_s}}\frac{h}{h_s^2}\overline{E_f}(\alpha_f - \alpha_s)\Delta T \tag{8}$$

where $\overline{E_s}$ and α_s are the biaxial modulus ($E_s/[1-\nu_s]$) and thermal expansion coefficient, respectively, of the Si substrate. Equation (8) is used for curvature evolution of the uniform passivation layer, which is a continuous SiO_2 layer in this work.

2.1. Unpassivated lines

The total strains during thermal excursions are the same along the Cu and SiO_2 lines, and they are related to the effective thermal expansion coefficient along the lines as

$$\alpha_x\Delta T = \frac{\langle\sigma_l\rangle}{E_l} + \alpha_l\Delta T = \frac{\langle\sigma_o\rangle}{E_o} + \alpha_o\Delta T \tag{9}$$

where $\langle\sigma_l\rangle$ and $\langle\sigma_o\rangle$ are the volume-averaged stresses in the Cu and SiO_2 lines, respectively. A force balance equation for this geometry, Fig. 1(a), gives

$$f_l\langle\sigma_l\rangle + f_o\langle\sigma_o\rangle = 0. \tag{10}$$

From equations (9) and (10), the effective thermal expansion coefficient along the line direction is

$$\alpha_x = \frac{f_l E_l\alpha_l + f_o E_o\alpha_o}{f_l E_l + f_o E_o}. \tag{11}$$

The effective elastic modulus along the line direction is written, using the composite theory, as

$$E_x = f_l E_l + f_o E_o. \tag{12}$$

Substituting E_x and α_x from equations (11) and (12) for the corresponding properties in equation (6), the curvature change along the lines, κ_x, is found to be

$$\kappa_x = \frac{6}{E_s}\frac{h}{h_s^2}E_x(\alpha_x - \alpha_s)\Delta T. \tag{13}$$

Across the lines, consideration of thermal expansion in the line and of the Poisson effect gives

$$\alpha_y\Delta T = f_l\left[-\nu_l\frac{\langle\sigma_l\rangle}{E_l} + \alpha_l\Delta T\right] + f_o\left[-\nu_o\frac{\langle\sigma_o\rangle}{E_o} + \alpha_o\Delta T\right]. \tag{14}$$

Substituting $\langle\sigma_l\rangle$ and $\langle\sigma_o\rangle$ from equations (9) and (10) into equation (14), the effective thermal expansion coefficient across the line direction is calculated as

$$\alpha_y = f_l\alpha_l + f_o\alpha_o + \frac{f_l f_o(\nu_l E_o - \nu_o E_l)(\alpha_l - \alpha_o)}{f_l E_l + f_o E_o}. \tag{15}$$

The effective elastic modulus across the line direction is written, with standard composite theory, as

$$E_y = \frac{E_l E_o}{f_l E_o + f_o E_l}. \tag{16}$$

Substituting E_y and α_y from equations (15) and (16) into equation (6), the curvature change across the lines, κ_y, becomes

$$\kappa_y = \frac{6}{E_s}\frac{h}{h_s^2}E_y(\alpha_y - \alpha_s)\Delta T. \tag{17}$$

Wikström *et al.* [9] derived expressions for the normal components of volume-averaged stresses in interconnect lines for two limiting cases: very low and high line aspect ratios, h/w. At a very low line aspect ratio, $h/w \to 0$, the interconnect structure can be considered as comprising individual Cu and SiO_2 films. Therefore, the curvature changes in both directions, i.e. along and across the lines, are the same and are obtained by adding the appropriate contribution from each film

$$\kappa_x^{low} = \kappa_y^{low} = -6\frac{h}{h_s^2}\frac{1-\nu_s}{E_s}[f_l\langle\sigma_l\rangle^{low} + f_o\langle\sigma_o\rangle^{low}] \tag{18}$$

where $\langle\sigma_l\rangle^{low}$ and $\langle\sigma_o\rangle^{low}$ are the volume-averaged biaxial stresses in the lines and the oxide, respectively, for the case of the low line aspect ratio. Similarly, κ_l^{low} and κ_o^{low} are the curvatures in the Cu and SiO_2 films, respectively.

As integration of the devices increases with decreasing line width, the aspect ratio of interconnect lines currently used in the semiconductor industry is also increased. At high line aspect ratios, $h/w \geq 1$, the curvature changes in each direction are obtained as follows:

$$\begin{bmatrix}\kappa_x^{high}\\ \kappa_y^{high}\end{bmatrix} = -6\frac{h}{h_s^2}\frac{1}{E_s}\begin{bmatrix}1 & -\nu_s\\ -\nu_s & 1\end{bmatrix} \times \begin{bmatrix}f_l\langle\sigma_{xx}^l\rangle^{high} + f_o\langle\sigma_{xx}^o\rangle^{high}\\ f_l\langle\sigma_{yy}^l\rangle^{high} + f_o\langle\sigma_{yy}^o\rangle^{high}\end{bmatrix} \tag{19}$$

where the superscript "high" denotes the high line

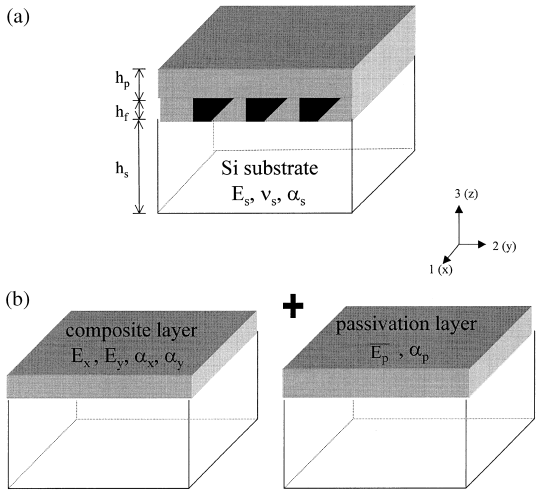

Fig. 2. Schematic of passivated Cu interconnect lines on a Si substrate following passivation: (a) actual interconnect structure; (b) superimposition of the composite layer and passivation layer.

aspect ratio for the components of volume-averaged stresses and curvatures in the Cu and SiO_2 lines in this regime. At $f_l = f_o = 0.5$, equations (13) and (17) give approximate values with less than 5% error compared with the values from equation (19). Therefore, the present model shows a reasonably good match in the range of practical line geometry, $h/w \geq 1$, in spite of its simplifying assumption that the curvatures along and across the line direction do not influence one another.

2.2. Passivated lines

The evolution of curvatures in passivated elastic Cu interconnect lines can also be assessed using the above simple model by invoking the concept of superposition. Figure 2 shows a schematic of passivated Cu lines, which can be regarded as superimposition of the composite layer and the passivation layer. For a given passivation material, the curvature change resulting from the passivation layer, κ_p, is obtained in terms of the biaxial modulus of the passivation layer, $\overline{E_p}$ $(= E_p/[1-\nu_p])$, its thermal expansion coefficient, α_p, and its thickness, h_p, using equation (8) as

$$\kappa_p = \frac{6}{\overline{E_s}} \frac{h_p}{h_s^2} \overline{E_p} (\alpha_p - \alpha_s) \Delta T. \tag{20}$$

By adding κ_p from equation (20) to κ_x and κ_y from equations (13) and (17), respectively, curvature changes of passivated lines, κ_x' and κ_y', are obtained:

$$\begin{aligned} \kappa_x' &= \kappa_x + \kappa_p \\ &= \frac{6}{E_s} \frac{h}{h_s^2} E_x (\alpha_x - \alpha_s) \Delta T + \frac{6}{\overline{E_s}} \frac{h_p}{h_s^2} \overline{E_p} (\alpha_p \\ &\quad - \alpha_s) \Delta T \end{aligned} \tag{21}$$

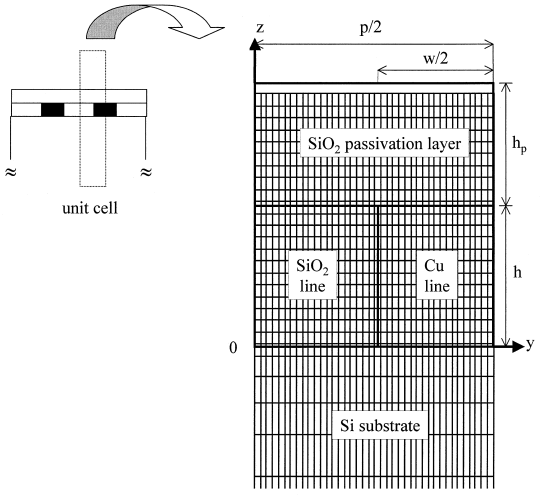

Fig. 3. A representative unit cell (top portion) and finite element discretization for Cu lines in the Damascene process.

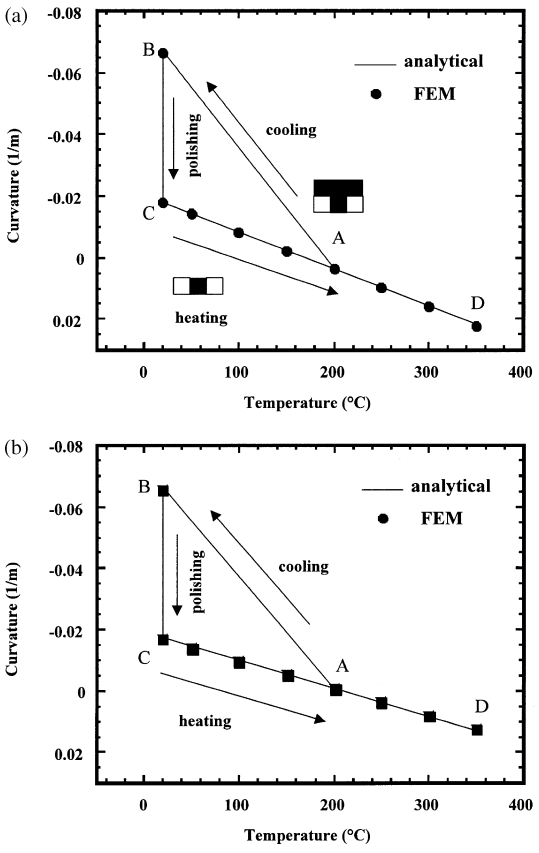

Fig. 4. Curvature changes of unpassivated Cu lines in the Damascene process at fixed line geometry ($h = 1$ μm, $h_s = 525$ μm, $h/w = 1$, $p/w = 2$). The Cu layer is deposited at 200°C: (a) along lines; (b) across lines.

$$\kappa_y' = \kappa_y + \kappa_p = \frac{6}{E_s}\frac{h}{h_s^2}E_y(\alpha_y - \alpha_s)\Delta T + \frac{6}{\overline{E_s}}\frac{h_p}{h_s^2}\overline{E_p}(\alpha_p - \alpha_s)\Delta T. \quad (22)$$

The accuracy of this result will be assessed in Section 4.

3. FINITE ELEMENT ANALYSIS

The finite element method (FEM) was used to verify the present analytical model. For this purpose, the general purpose finite element program ABAQUS [10] was employed. The mesh used in the present numerical simulation is shown in Fig. 3. Due to the periodicity and symmetry of the arrangement, only a unit segment ranging from a symmetric axis and the neighboring periodic boundary is needed. Here h, w, and p represent the height, width, and spacing of Cu lines, respectively. A generalized plane strain formulation, which is an extension of the plane strain framework (with the y–z plane being the plane of deformation), was used in the calculations. This was accomplished by superimposing a longitudinal strain, ε_{xx}, on the plane strain state. The detailed procedure for obtaining the curvatures using such numerical simulation can be found in earlier papers [11, 12].

Table 1 shows the material properties used in the simulations [12, 13]. Isotropic material properties were used, and residual stresses which may result from Cu deposition and/or polishing were not taken into account. This analysis deals with only elasticity, which is expected to be valid over a wide range of practical interest since the material surrounding the Cu lines, especially in the case of passivated lines, leads to elevated levels of hydrostatic stress in the lines thereby inducing constrained deformation [6]†.

4. RESULTS AND DISCUSSION

4.1. Changes in curvature during the Damascene process

Figure 4(a) shows curvature changes along the unpassivated Cu lines from the Damascene process for a fixed line geometry ($h/w = 1$, $p/w = 2$). First we assume that the SiO_2 layer is grown by thermal oxidation at 1000°C, cooled down to 200°C, and then patterned into trenches (at A). The residual stress formed during oxidation is not considered in this simulation. At 200°C, a Cu layer is deposited on patterned SiO_2 lines, and then cooled down to room temperature (A→B). A very large curvature change occurs during cooling in this direction. When an excess Cu layer (1 μm thick) is removed by polishing (B→C), the curvature drops drastically. Then as the temperature is raised from room temperature (C→D), the curvature changes in the opposite direction. Across the lines, Fig. 4(b), the curvature change shows different slopes from those along lines during cooling and heating. Analytical predictions (Equations (13) and (17) for unpassivated lines and equations (21) and (22) for the case

Table 1. Material properties used in the simulations

	E (GPa)	ν	α (10^{-6}/°C)
Si	130	0.28	2.60
Cu	110	0.30	17.0
SiO_2	71.4	0.16	0.524

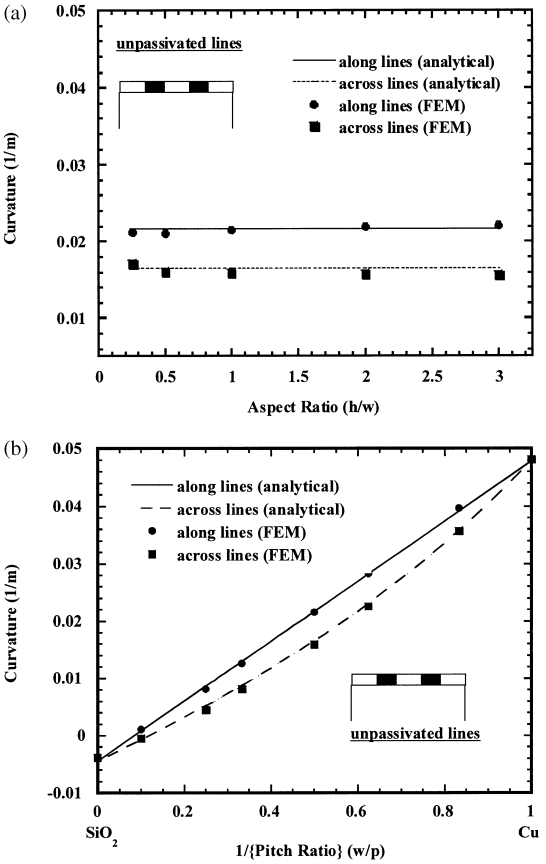

Fig. 5. Curvature changes of unpassivated Cu lines ($h = 1$ μm, $h_s = 525$ μm) during heating from room temperature to 200°C as a function of: (a) aspect ratio at fixed pitch ratio ($p/w = 2$); (b) reciprocal of pitch ratio at fixed aspect ratio ($h/w = 1$).

† In the unpolished Cu layer (before CMP), however, plastic deformation can occur because the yield strength of unpassivated Cu films can be very low at moderate temperature (well below 400°C) [14]. Unpassivated Cu lines (after CMP) which are in the trench with its top face being free may also plastically deform due to high deviatoric components unless the aspect ratio is very high. These inelastic deformations should be considered when experimental data are compared with the present model.

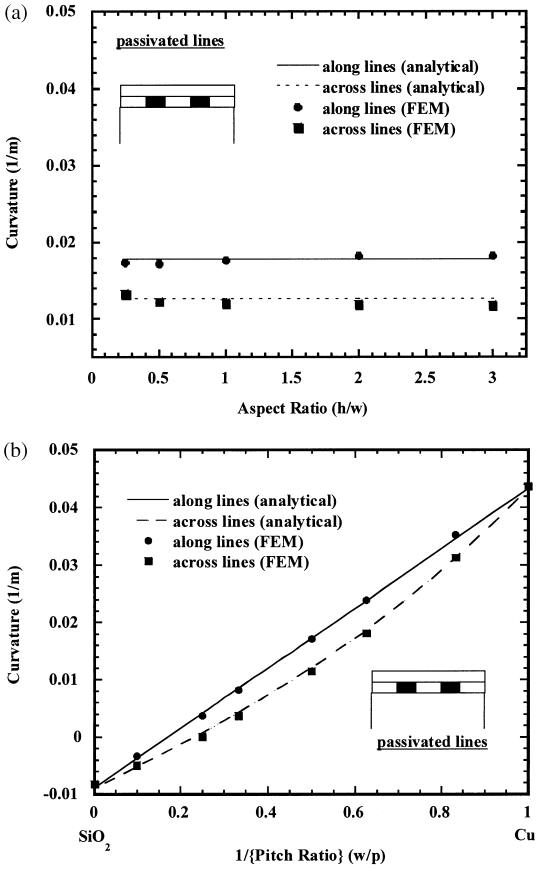

Fig. 6. Curvature changes of passivated Cu lines with SiO_2 passivation layer ($h = 1$ μm, $h_p = 1$ μm, $h_s = 525$ μm) during heating from room temperature to 200°C as a function of: (a) aspect ratio at fixed pitch ratio ($p/w = 2$); (b) reciprocal of pitch ratio at fixed aspect ratio ($h/w = 1$).

with excess Cu.) are exactly matched with calculated values by FEM in both directions during the above fabrication and thermomechanical processes.

4.2. *Effects of line and passivation geometry*

Figure 5(a) shows curvature changes during heating from room temperature to 200°C as a function of aspect ratio at a fixed pitch ratio ($p/w = 2$). When the pitch ratio is fixed, the fraction of Cu in this composite layer is unchanged. Therefore, equations (13) and (17) give constant curvature values, which reasonably fit the results of numerical simulation over a wide range.

Figure 5(b) shows curvature changes during heating from room temperature to 200°C as a function of the reciprocal of pitch ratio (w/p), which corresponds to the volume fraction of Cu, at fixed aspect ratio ($h/w = 1$). As the spacing between the Cu lines increases, the fraction of Cu in this layer decreases. Considering the volume fraction in equations (13) and (17), analytical values agree closely with FEM results over all Cu volume fraction in the layer which consists of Cu and SiO_2 lines. When a pure Cu film is considered ($w/p \rightarrow 1$), the present one-dimensional model gives

$$\kappa_x = \kappa_y = \frac{6}{E_s}\frac{h}{h_s^2}E_l(\alpha_l - \alpha_s)\Delta T. \tag{23}$$

However, the biaxial modulus of the Cu film and the Si substrate should be used to obtain exact curvature changes for this two-dimensional structure:

$$\kappa_x^{\text{exact}} = \kappa_y^{\text{exact}} = \frac{6}{\overline{E_s}}\frac{h}{h_s^2}\overline{E_l}(\alpha_l - \alpha_s)\Delta T$$

$$= \left[\frac{1-\nu_s}{1-\nu_l}\right]\frac{6}{E_s}\frac{h}{h_s^2}E_l(\alpha_l - \alpha_s)\Delta T. \tag{24}$$

Therefore, the factor of $(1-\nu_s)/(1-\nu_l)$ can be regarded as an error of the present model in this limiting case, and it gives only 3% error for the pure Cu film. In the same way, the corresponding factor for a pure SiO_2 film, ($w/p \rightarrow 0$), can be expressed as $(1-\nu_s)/(1-\nu_o)$, which shows a 17% error. But since this SiO_2 rich region shows very small curvature changes compared with that with high Cu volume fraction, this error is not large in an absolute value. Therefore, it shows a very good agreement with numerical simulation in a fairly wide range, where practical interconnect line geometries lie.

Analytical predictions and FEM results for passivated lines with SiO_2 passivation layer are shown in Fig. 6. They represent almost the same trends as unpassivated lines with smaller absolute values because the thermal expansion coefficient of oxide is lower than Si substrate. Due to the high diffusivity of Cu through SiO_2 and Si, a diffusion barrier such as TaN is commonly employed [7]. Although it makes more complicated interconnect structures, the effect of this additional layer can be easily incorporated in the present model by superimposition for linear elasticity condition and may be negligible if this layer is very thin, i.e. of the order of a few hundred Ångströms.

5. CONCLUSIONS

In this paper, a simple analytical model based on a composite analogy has been used to predict curvature in unpassivated and passivated Cu lines in the Damascene process. A layer consisting of copper and oxide lines is modeled as a homogenized composite layer consisting of Cu and SiO_2 lines. The effective thermoelastic properties of the composite layer are computed in terms of volume fractions and thermoelastic properties of each line using standard composite theory, which enables us to calculate curvature changes during the Damascene process employing thermal cycling and polishing. Finite element analyses have been used to assess the accuracy of the simple analytical model. These

values are exactly matched with each other during Cu deposition, polishing, passivation, and thermal cycling under the assumption of isotropic material properties and linear elasticity conditions. Although residual stresses are not incorporated into the analyses, they can be appropriately superimposed to modify the predicted curvatures if the magnitudes of residual stresses are known. The effects of line geometry such as aspect ratio, h/w, and pitch ratio, p/w, can also be rationalized with the present model. In addition, the model can also be easily extended to include passivated copper lines, for any passivation material, by superimposing the curvature change resulting from an additional layer.

Acknowledgements—This work was supported by the Office of Naval Research under Grant N-0014-94-1-0139 to MIT. The authors acknowledge helpful discussions with A. Wikström and Y.-L. Shen.

REFERENCES

1. Korhonen, M. A., Børgesen, P., Tu, K. N. and Li, C.-Y., *J. appl. Phys.*, 1993, **73**, 3790.
2. Clement, J. J. and Thompson, C. V., *J. appl. Phys.*, 1995, **78**, 900.
3. Gleixner, R. J., Clemens, B. M. and Nix, W. D., *J. Mater. Res.*, 1997, **12**, 2081.
4. Greenbaum, B., Sauter, A. I., Flinn, P. A. and Nix, W. D., *Appl. Phys. Lett.*, 1991, **58**, 1845.
5. Børgesen, P., Lee, J. K., Gleixner, R. and Li, C.-Y., *Appl. Phys. Lett.*, 1992, **60**, 1706.
6. Moske, M. A., Ho, P. S., Mikalsen, D. J., Cuomo, J. J. and Rosenberg, R., *J. appl. Phys.*, 1993, **74**, 1716.
7. Hu, C.-K., Luther, B., Kaufman, F. B., Hummel, J., Uzoh, C. and Pearson, D. J., *Thin Solid Films*, 1995, **262**, 84.
8. Timoshenko, S., in *Strength of Materials*, 3rd edn. Krieger, Huntington, NY, 1976, p. 88.
9. Wikström, A., Gudmundson, P. and Suresh, S., *J. appl. Phys.*, 1999, **86**, 6088.
10. ABAQUS Version 5. 8, general purpose finite element program, Hibbit, Karlson and Sorensen Inc., Pawtucket, RI, 1999.
11. Shen, Y.-L., Suresh, S. and Blech, I. A., *J. appl. Phys.*, 1996, **80**, 1388.
12. Gouldstone, A., Shen, Y.-L., Suresh, S. and Thompson, C. V., *J. Mater. Res.*, 1998, **13**, 1956.
13. Wikström, A., Gudmundson, P. and Suresh, S., *J. Mech. Phys. Solids*, 1999, **47**, 1113.
14. Shen, Y.-L., Suresh, S., He, M. Y., Bagchi, A., Kienzle, O., Rühle, M. and Evans, A. G., *J. Mater. Res.*, 1998, **13**, 1928.